Singularity Analysis of Closed-Loop Kinematic Chains

Article *in* IEEE Transactions on Robotics and Automation · July 1990

DOI: 10.1109/70.56660 · Source: IEEE Xplore

2 authors:

Clément Gosselin
Université Laval
705 PUBLICATIONS **30,911** CITATIONS
SEE PROFILE

Jorge Angeles
McGill University
542 PUBLICATIONS **16,281** CITATIONS
SEE PROFILE

Singularity Analysis of Closed-Loop Kinematic Chains

Clément Gosselin
Département de Génie Mécanique
Université Laval
Québec, Québec, Canada

and

Jorge Angeles
Department of Mechanical Engineering
and
McGill Research Center for Intelligent Machines
McGill University
817 Sherbrooke St. West
Montréal, Québec, Canada H3A 2K6

March 22nd 1989
Revised July 17th 1989

Manuscript accepted for publication in
The IEEE TRANSACTIONS ON ROBOTICS AND AUTOMATION

Abstract

This paper presents an analysis of the different kinds of singularities encountered in closed-loop kinematic chains. A general classification of these singularities in three main groups, which is based on the properties of the Jacobian matrices of the chain, is described. The identification of the singular configurations is particularly relevant for hard automation modules or robotic devices based on closed kinematic chains, such as linkages and parallel manipulators. Examples are given to illustrate the application of the method to these mechanical systems.

1 Introduction

The study of the kinematics of mechanical systems leads inevitably to the problem of singular configurations. These configurations are defined as those in which the Jacobian matrices involved, i.e., those matrices relating the input speeds with the output speeds, become rank deficient. They correspond to configurations of the system that are usually undesirable since the degree of freedom of the system changes instantaneously.

For simple, open chains, the singularity problem has been addressed by several authors [1–8]. For complex chains, i.e., kinematic chains containing multiple loops and many degrees of freedom, studies are scarce [9]. However, the problem in this context is essentially the same as that encountered in single-degree-of-freedom, simple, closed kinematic chains [10–14].

A singularity analysis for closed-loop kinematic chains is presented in this paper. It is shown that the singularities encountered in closed-loop kinematic chains can be divided into three main groups. This classification, in fact, completes and formalizes observations that were made in [14], where singularities of two different natures were identified for a closed-loop manipulator. Moreover, the singularities discussed here, which have been known under different names, have been studied by several authors, particularly in connection with mechanisms; see for instance [13, 15–20]. The purpose of the analysis presented here is to introduce a general classification of singularities that is well suited for robotic devices and that includes other considerations that are particularly relevant to these machines. As demonstrated by the examples included here, this analysis is applicable to simple and complex kinematic chains in general. Complex kinematic chains are defined as the ones containing at least one link that is directly coupled to at least three other links.

The possibility of applications of simple and complex closed kinematic chains are numerous. Examples can be found even in the early work on machinery. The Watt and Stephenson linkages, for instance, clearly constitute planar 6-link complex kinematic chains [13,18]. Parallel manipulators probably constitute the best known example of complex kinematic chains used in robotics. However, more recently, with the advances in computer-aided synthesis of linkages, researchers have started to consider the use of complex kinematic chains as hard automation modules which are designed to perform a precise repetitive task. The inherent rigidity of complex kinematic chains is one of the important motivations behind these studies, because complex architectures enhance both the accuracy and the load-carrying ca-

pacity of the systems at hand. Some of the designs even include a certain functional flexibility, i.e., provision to perform alternate tasks by a simple change—which can be done within minutes or even seconds—in their linkage parameters; for instance, changing the distance or angle between two joint axes of the fixed link provides a reconfigurability that adds to the system functionality. Examples of the results obtained with this approach are found in [21].

The emergence of these new mechanisms and manipulators based on closed-loop kinematic chains motivates the singularity analysis presented here, which will be illustrated through a series of examples.

2 Singularity Analysis

A closed-loop kinematic chain consists of a set of rigid bodies connected to each other with joints and where at least one closed loop exists. The chain is also characterized by a set of inputs, denoted here by an n-dimensional vector θ, which correspond to the powered joints and by a set of output coordinates, denoted here by an m-dimensional vector $\mathbf{x}$. These input and output vectors depend on the nature and purpose of the kinematic chain. For instance, in a parallel manipulator, the input vector θ represents the set of actuated joints and the output vector $\mathbf{x}$ represents the Cartesian coordinates of the gripper. However, in general, the output need not be a set of Cartesian coordinates and can also correspond to joint angles or displacements. Furthermore, although the number of inputs and outputs does not have to be equal, the number of independent inputs and outputs will always be the same, except in the presence of redundancies [22], and, therefore, vectors θ and $\mathbf{x}$ can be assumed to be of the same dimension which will be equal to the degree of freedom of the linkage, say n. The relationship between the input and output coordinates is then written as

$$\mathbf{F}(\theta, \mathbf{x}) = \mathbf{0} \qquad \text{x=f(θ)} \tag{1}$$

where $\mathbf{F}$ is an n-dimensional implicit function of θ and $\mathbf{x}$, and $\mathbf{0}$ is the n-dimensional zero vector. Differentiating eq.(1) with respect to time leads to the relationship between the input and output speeds as follows:

$$\mathbf{A}\dot{\mathbf{x}} + \mathbf{B}\dot{\theta} = \mathbf{0} \tag{2}$$

where

$$\mathbf{A} = \frac{\partial \mathbf{F}}{\partial \mathbf{x}}, \qquad \mathbf{B} = \frac{\partial \mathbf{F}}{\partial \theta}, \tag{3}$$

and where $\mathbf{A}$ and $\mathbf{B}$ are both $n \times n$ Jacobian matrices. Matrices $\mathbf{A}$ and $\mathbf{B}$ are, of course, configuration dependent, i.e., $\mathbf{A} = \mathbf{A}(\mathbf{x}, \theta)$ and $\mathbf{B} = \mathbf{B}(\mathbf{x}, \theta)$.

As stated above, singularities occur in configurations where either $\mathbf{A}$ or $\mathbf{B}$ becomes singular. Thus, for general closed-loop kinematic chains, a distinction can be made between three kinds of singularities which have different physical interpretations.

(i) The first kind of singularity occurs when the following condition is verified:

$$\det(\mathbf{B}) = 0 \tag{4}$$

The corresponding configuration is one in which the chain reaches either a boundary of its workspace, or an internal boundary limiting different subregions of the workspace where the number of branches is not the same. In other words, this kind of singularity consists of *the set of points where different branches of the inverse kinematic problem meet*, the inverse kinematic problem being understood here as the computation of the values of the input variables from given values of the output variables. Since the nullity of $\mathbf{B}$—the dimension of its nullspace—is nonzero in the presence of a singularity of the first kind, we can find nonzero vectors $\dot{\theta}$ for which $\dot{\mathbf{x}}$ will be equal to zero and, therefore, some of the velocity vectors $\dot{\mathbf{x}}$ cannot be produced at the output. Typically, these would be velocities orthogonal to the boundary and directed towards the outside of the workspace. In such a configuration, we say that the output link loses one or more degrees of freedom and, in virtue of the series-parallel dualities [19], this implies that the output link can resist one or more forces or moments without exerting any torque—or force—at the powered joints. If the kinematic chain considered is a mechanism, the first kind of singularity corresponds to a configuration in which the output link is at a deadpoint.

(ii) The second kind of singularity occurs when we have the following:

$$\det(\mathbf{A}) = 0 \tag{5}$$

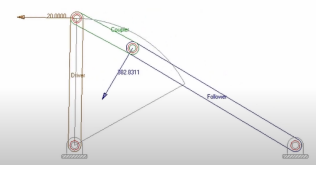

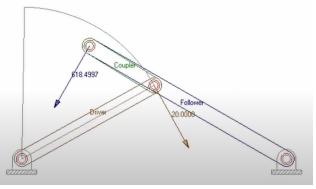

This corresponds to configurations in which the gripper is locally movable even when all the actuated joints are locked. As opposed to the first one, this kind of singularity lies within the workspace of the chain and corresponds to *a point or a set of points where different branches of the direct kinematic problem meet*. In the direct kinematic problem, it is desired to obtain the values of the output variables from given values of the input variables. Since in this case the nullspace of $\mathbf{A}$ is not empty, there exists nonzero output rate vectors $\dot{\mathbf{x}}$ which are mapped into the origin by $\mathbf{A}$, i.e., which will correspond

to a velocity of zero of the input joints. In such a configuration, we say that the output link gains one or more degrees of freedom and, in virtue of the series-parallel dualities [19], this implies that the output link cannot resist one or more forces or moments even when all actuators are locked. If the kinematic chain considered is a mechanism, the second kind of singularity corresponds to a configuration in which the input link is at a deadpoint.

Both the first and second kinds of singularities correspond to *configurations* that can happen in a general complex kinematic chain.

(iii) The third kind of singularity is of a slightly different nature than the first two, since it requires conditions on the linkage parameters. This occurs when, for certain configurations, both $\mathbf{A}$ and $\mathbf{B}$ become simultaneously singular. If some specific conditions on the linkage parameters are satisfied, the chain can reach configurations where the position relation, given by eq.(1), degenerates. This corresponds to configurations in which the chain can undergo finite motions when its actuators are locked or in which a finite motion of the inputs produces no motion of the outputs such as, for example, a linkage having a constant branch [23]. For linkages having a quadratic input-output equation, such as the planar and spherical four-bar linkages and the spatial $RSSR$ linkage [24], the third kind of singularity corresponds to a case for which all three coefficients of the quadratic equation are equal to zero, for a particular set of configurations. This degeneracy is illustrated with a planar four-bar linkage in Fig. 1.

The three kinds of singularities will now be illustrated with some examples of simple and complex closed-loop kinematic chains.

3 Example 1: Planar $RRRP$ Mechanism

A planar $RRRP$ mechanism is shown in Fig. 2. This one-degree-of-freedom mechanism is often referred to as a crank-slider four-bar linkage. Let us consider the crank angle θ as the input variable and the displacement of the slider, denoted as x, as the output. In this case, since we have only one input and one output, the Jacobian matrices are 1×1 matrices, i.e., scalars, and will be denoted as A and B. From the geometry of the linkage, we can write:

$$x = R\cos\theta + l\cos\psi \tag{6}$$

and

$$R\sin\theta = l\sin\psi \tag{7}$$

or

$$\cos\psi = \pm\sqrt{1 - \frac{R^2}{l^2}\sin^2\theta} \tag{8}$$

substitution of eq.(8) into eq.(6) leads to:

$$x = R\cos\theta \pm l\sqrt{1 - r^2\sin^2\theta} \tag{9}$$

where

$$r \equiv \frac{R}{l} \tag{10}$$

The double sign thus being consistent with the fact that the direct kinematic problem has two branches. Upon differentiation of eq.(9) with respect to time, one obtains:

$$A\dot{x} + B\dot{\theta} = 0 \tag{11}$$

where

$$A = \sqrt{1 - r^2\sin^2\theta}, \quad B = -R\sin\theta\left(\sqrt{1 - r^2\sin^2\theta} \pm r\cos\theta\right) \tag{12}$$

r^2 ???

Therefore, the first kind of singularity arises when $B = 0$, i.e., when $\theta = 0$ or π. In this configuration, eq.(9) becomes:

$$x = \pm R \pm l \tag{13}$$

and the links of length R and l are aligned, which corresponds to the limit of the workspace. Since B is equal to zero, the value of $\dot{x}$ will be equal to zero, whatever the value of $\dot{\theta}$ is. Moreover, a force applied at the output along the direction of the links will have no effect on the input.

The second kind of singularity occurs when $A = 0$. This condition leads to:

$$\sin\theta = \frac{l}{R} \tag{14}$$

The corresponding configuration is shown in Fig. 3. This configuration is clearly within the range of motion of the output, i.e., within the workspace. Moreover, since the second term of eq.(9) vanishes, the two branches of the direct kinematic problem meet. The output can undergo infinitesimal motion even if the input is locked. Moreover, the mechanism cannot resist a force applied at the output along the x axis.

As stated above, the third kind of singularity requires that certain conditions on the linkage parameters be satisfied. For the example treated here, the condition is that the input and coupler links have the same length, i.e.,

$$R = l \tag{15}$$

Under this assumption, eq.(9) can be rewritten as:

$$x = R\cos\theta \pm R\cos\theta \tag{16}$$

or

$$x = \begin{cases} 0 \\ 2R\cos\theta \end{cases} \tag{17}$$

which clearly shows that the mechanism has a constant branch. Therefore, when x is equal to zero, the input can undergo arbitrary rotations while the output remains at rest and the first two kinds of singularities can meet. This situation is represented in Fig. 4.

4 Example 2: The Watt Linkage

A linkage of this type is shown in Fig. 5. The mechanism has one degree of freedom, and the input and output variables are angles θ and ϕ, respectively. Again, the Jacobian matrices are scalar quantities.

From the geometry of the linkage, we can write:

$$x_1 = -\cos(\psi + \pi/3) \tag{18}$$

and

$$y_1 = \frac{\sqrt{3}}{2} + \sin(\psi + \pi/3) \tag{19}$$

and also:

$$\alpha = \tan^{-1}\left(\frac{y_1}{x_1'}\right) \tag{20}$$

where

$$x_1' = x_1 - 1/2 \tag{21}$$

and

$$\beta = \tan^{-1}\left(\frac{l_1\sin\theta - \sqrt{3}/2}{l_1\cos\theta + 1/2}\right) \tag{22}$$

Moreover, using the *law* of cosines, we obtain:

$$l_4^2 = l_3^2 + {x_1'}^2 + y_1^2 - 2l_3\sqrt{{x_1'}^2 + y_1^2}\cos(\alpha - \phi) \tag{23}$$

and

$$\begin{aligned} l_2^2 &= 1 + (l_1\cos\theta + 1/2)^2 + (l_1\sin\theta - \sqrt{3}/2)^2 \\ &\quad -2\sqrt{(l_1\cos\theta + 1/2)^2 + (l_1\sin\theta - \sqrt{3}/2)^2}\cos(\psi - \beta) \end{aligned} \tag{24}$$

Given a certain value of the input angle θ, angle ψ can be computed from eqs.(22) and (24) and then angle ϕ is obtained from eqs.(20), (21) and (23). Upon differentiation of these equations with respect to time, the following is obtained:

$$\dot{\psi} = (C_1 + C_2)\dot{\theta} \tag{25}$$

where

$$C_1 = \frac{(\sqrt{3}l_1\sin\theta - l_1\cos\theta - l_1^2)(-1/2l_1\sin\theta - \sqrt{3}/2l_1\cos\theta)}{2\sin(\psi - \beta)[(1/2 + l_1\cos\theta)^2 + (l_1\sin\theta - \sqrt{3}/2)^2]^{3/2}} \tag{26}$$

and

$$C_2 = \frac{l_1^2 + 1/2l_1\cos\theta - \sqrt{3}/2l_1\sin\theta}{(l_1\cos\theta + 1/2)^2 + (l_1\sin\theta - \sqrt{3}/2)^2} \tag{27}$$

As well,

$$\dot{\phi} = C_1'\dot{x}_1 + C_2'\dot{y}_1 \tag{28}$$

where

$$C_1' = \frac{-y_1}{{x_1'}^2 + y_1^2} + \frac{x_1'({x_1'}^2 + y_1^2 + l_4^2 - l_3^2)}{2l_3\sin(\alpha - \phi)({x_1'}^2 + y_1^2)^{3/2}} \tag{29}$$

and

$$C_2' = \frac{x_1'}{{x_1'}^2 + y_1^2} + \frac{y_1({x_1'}^2 + y_1^2 + l_4^2 - l_3^2)}{2l_3\sin(\alpha - \phi)({x_1'}^2 + y_1^2)^{3/2}} \tag{30}$$

Therefore, the relation between the input and output velocities can be written as:

$$A\dot{\phi} + B\dot{\theta} = 0 \tag{31}$$

where

$$A = D_1D_2, \quad B = N_1N_2 \tag{32}$$

with

$$
\begin{aligned}
N_1 &= (l_1\cos\theta - \sqrt{3}l_1\sin\theta + l_1^2 + l_2^2)(1/2l_1\sin\theta + \sqrt{3}/2l_1\cos\theta) \\
&\quad +2\sin(\psi-\beta)(l_1^2 + 1/2l_1\cos\theta - \sqrt{2}/2l_1\sin\theta) \\
&\quad \times\sqrt{1-\sqrt{3}l_1\sin\theta + l_1\cos\theta + l_1^2} \qquad (33)\\
N_2 &= \sin\psi({x'_1}^2 + y_1^2 + l_4^2 - l_3^2) \\
&\quad +2l_3\sin(\alpha-\phi)(1+\cos\psi)\sqrt{{x'_1}^2 + y_1^2} \qquad (34)\\
D_1 &= 2\sin(\psi-\beta)(1-\sqrt{3}l_1\sin\theta + l_1\cos\theta + l_1^2)^{3/2} \qquad (35)\\
D_2 &= 2l_3\sin(\alpha-\phi)({x'_1}^2 + y_1^2)^{3/2} \qquad (36)
\end{aligned}
$$

The first kind of singularity occurs when $B = 0$, i.e., when

$$N_1 = 0 \qquad \text{or} \qquad N_2 = 0 \tag{37}$$

The first condition corresponds to the set of configurations in which links l_1 and l_2 are aligned, which clearly defines a boundary of the workspace. The second condition corresponds to configurations where link l_4 is aligned with the line connecting joints 4 and 5, which again defines a limit position of the output link. In these configurations, the velocity of the output is always zero, whatever the input velocity is.

The second kind of singularity, i.e., the one in which the velocity of the output link can be nonzero even if the input velocity vanishes, occurs here when A is equal to zero, i.e.:

$$D_1 = 0 \qquad \text{or} \qquad D_2 = 0 \tag{38}$$

The first condition can be rewritten as:

$$\sin(\psi - \beta) = 0 \tag{39}$$

which corresponds to configurations in which link l_2 is aligned with the line connecting joints 3 and 4. This kind of configuration is shown in Fig. 6, where it is clear that the output link can undergo an infinitesimal motion even if the input is locked. The second condition can, in turn, be rewritten as:

$$\sin(\alpha - \phi) = 0 \tag{40}$$

which corresponds to configurations in which links l_3 and l_4 are aligned.

The conditions on the link lengths required for the third kind of singularity are given by the following:

$$l_1 = l_2 = 1 \qquad \text{or} \qquad l_3 = l_4 = 1 \tag{41}$$

When the first equality above is verified, the mechanism can reach configurations where joints 2 and 4 are superimposed, and the output can then undergo finite motions while the input is at rest. As a matter of fact, since links l_1 and l_2 are aligned with the lines connecting joints 1 and 4 and joints 3 and 4, respectively, they become kinematically irrelevant and the whole linkage is reduced to a four-bar planar linkage.

On the other hand, if the second equality of eq.(41) is verified, the mechanism can reach configurations where joints 4 and 6 are superimposed. In this case, links l_3 and l_4 become irrelevant and the linkage has a constant branch, i.e., a branch on which the output link remains at rest.

5 Example 3: Planar Three-Degree-of-Freedom Manipulator with Revolute Actuators

A planar parallel manipulator is represented in Fig. 7, all of whose joints are of the revolute type, and the three motors M_1, M_2, M_3 are fixed. The manipulator consists of a kinematic chain with three closed loops, namely M_1DABEM_2, M_2EBCFM_3, and M_3FCADM_1, the gripper being rigidly attached to triangle ABC. It is pointed out here that only two of the aforementioned loops are kinematically independent according to the definition given in [22].

This manipulator was studied in detail in [25]. It is assumed here that the manipulator is symmetric and therefore, the motors will be located on the vertices of an equilateral triangle and the link lengths will be the same for each leg, i.e.,

$$l_i = l'_i = l''_i, \quad i = 1, 2, 3 \tag{42}$$

Moreover, in what follows, the distance between any two of the motors will be set equal to unity, for normalization purposes. Triangle ABC will be referred to as *the gripper*, for it is kinematically equivalent to this. It is now recalled, from [25] that the following relation holds:

$$\mathbf{A}\dot{\mathbf{s}} + \mathbf{B}\dot{\theta} = \mathbf{0} \tag{43}$$

where $\dot{\theta} = [\dot{\theta}_1, \dot{\theta}_2, \dot{\theta}_3]^T$ is the vector of joint rates and $\dot{\mathbf{s}} = [\dot{x}, \dot{y}, \dot{\phi}]^T$ is the vector of Cartesian velocities. Moreover, $\mathbf{A}$ and $\mathbf{B}$ are the following:

$$\mathbf{A} = \begin{bmatrix} a_1 & b_1 & c_1 \\ a_2 & b_2 & c_2 \\ a_3 & b_3 & c_3 \end{bmatrix}, \quad \mathbf{B} = \mathrm{diag}(d_1, d_2, d_3) \tag{44}$$

where, for $i = 1, 2, 3$,

$$\begin{aligned} a_i &= 2l_1 y_{2i} \sqrt{x_{2i}^2 + y_{2i}^2} \sin\psi_i + \gamma_i E_i x_{2i} && (45)\\ b_i &= -2l_1 x_{2i} \sqrt{x_{2i}^2 + y_{2i}^2} \sin\psi_i + \gamma_i E_i y_{2i} && (46)\\ c_i &= 2l_1 l_3 \sqrt{x_{2i}^2 + y_{2i}^2} \sin\psi_i (x_{2i}\cos\phi_i + y_{2i}\sin\phi_i) \\ &\quad + \gamma_i E_i l_3 (x_{2i}\sin\phi_i - y_{2i}\cos\phi_i) && (47)\\ d_i &= 2l_1 (x_{2i}^2 + y_{2i}^2)^{3/2} \sin\psi_i && (48) \end{aligned}$$

variables E_i and ϕ_i being defined, for $i = 1, 2, 3$, as

$$E_i = l_2^2 - l_1^2 + x_{2i}^2 + y_{2i}^2 \tag{49}$$

$$\begin{aligned} \phi_1 &= \phi + \pi/6 && (50)\\ \phi_2 &= \phi + 5\pi/6 && (51)\\ \phi_3 &= \phi - \pi/2 && (52) \end{aligned}$$

with

$$\begin{aligned} \psi_i &= \cos^{-1}\left[\frac{l_1^2 - l_2^2 + x_{2i}^2 + y_{2i}^2}{2l_1\sqrt{x_{2i}^2 + y_{2i}^2}}\right] && (53)\\ x_{2i} &= x - l_3\cos\phi_i - x_{oi} && (54)\\ y_{2i} &= y - l_3\sin\phi_i - y_{oi} && (55) \end{aligned}$$

where (x_{oi}, y_{oi}) are the coordinates of the center of the ith motor. Moreover,

$$\gamma_i = \pm 1 \tag{56}$$

is a factor that depends on the branch we chose for the ith leg in the solution of the inverse kinematic problem.

The potential applications of this manipulator include pick-and-place operations over a planar surface, machining of planar surfaces, mobile bases

for a spatial manipulator and moving platforms for a terrestrial vehicle simulator.

The three kinds of singularities discussed above are now derived for this manipulator and the physical significance of each of these types of singularities is presented.

It is recalled that the first kind of singularity corresponds to the limit of the workspace and that it occurs when the determinant of $\mathbf{B}$ vanishes. This condition is encountered here when one of the diagonal entries of $\mathbf{B}$ vanishes, i.e., when

$$d_i = 0, \qquad i = 1 \text{ or } 2 \text{ or } 3 \tag{57}$$

From eq.(48), either of these leads to:

$$\sin \psi_i = 0 \ , \qquad i = 1 \text{ or } 2 \text{ or } 3 \tag{58}$$

This type of configuration is reached whenever the links of lengths l_1 and l_2 of one of the legs are aligned, as one can readily infer by inspection of Fig. 7. Moreover, since the solution of the inverse kinematic problem leads to two branches per leg, the corresponding quadratic equation leads to two solutions when the input Cartesian coordinates are located inside the workspace of the manipulator and to no real solution when the prescribed Cartesian coordinates are not within the workspace. Therefore, the limit of the workspace is defined by the set of points for which the quadratic equation will lead to only one solution, i.e., when we have the following condition:

$$\psi_i = \pm n\pi, \qquad n = 0, 1, 2, \ldots \qquad i = 1 \text{ or } 2 \text{ or } 3 \tag{59}$$

which is equivalent to eq.(58). Since in this type of configuration the ith leg is fully extended or folded, the set of Cartesian velocities of the gripper that correspond to a velocity of the point of attachment of the ith leg to the gripper along the folded or extended leg cannot be produced. This set of Cartesian velocities is given by the set of rotations of the gripper about an arbitrary point of a line passing through the ith point of attachment of the gripper and orthogonal to the ith leg. Moreover, a force applied at the gripper along the direction of the pair of aligned links will not affect the actuators.

The second kind of singularity, which is located inside the workspace of the manipulator, occurs when the determinant of $\mathbf{A}$ vanishes. For this type of configuration, there exists nonzero Cartesian velocities $\dot{\mathbf{s}}$ which are mapped into the zero vector by $\mathbf{A}$. These Cartesian velocities are then

possible even when the rates of all motors are zero. These configurations can be inferred from eq.(44) by imposing the linear dependence of the columns of $\mathbf{A}$, i.e.,

$$k_1 a_i + k_2 b_i + k_3 c_i = 0, \qquad i = 1, 2, 3 \tag{60}$$

for some real values of k_1, k_2, and k_3 not all of them zero.

By inspection of eqs.(60) and (45–47), two different cases for which the condition given by eq.(60) is satisfied can be identified. The first one is obtained when the lines along each of the three links of length l_2 intersect. In this case, we have

$$c_1 = c_2 = c_3 = 0 \tag{61}$$

and hence, eq.(60) can be satisfied with $k_1 = k_2 = 0$ and arbitrary k_3. The last column of the Jacobian matrix is equal to zero and hence, the nullspace of $\mathbf{A}$ is spanned by $[0,\, 0,\, 1]^T$. This nullspace corresponds here to the set of pure rotations of the gripper about its centroid. This set of velocity vectors will produce motor rates of zero, due to the transitory additional degree of freedom. A configuration of this type is shown in Fig. 8. Again, in virtue of the series-parallel dualities [19], the manipulator will not be able to withstand a torque applied at the gripper.

The second case for which eq.(60) can be verified is the set of configurations for which the three links of length l_2 are parallel. Indeed, by inspection of eqs.(45–46), we can define a set of vectors $\mathbf{v}_i$, $i = 1, 2, 3$, as the following two-dimensional vectors:

$$\mathbf{v}_i = [a_i,\, b_i]^T \tag{62}$$

where it is clear that $\mathbf{v}_i$ is the vector connecting the joint common to links l_1 and l_2 of the ith leg to the point of attachment of link l_2 of the same leg to the gripper, i.e., $\mathbf{v}_i$ is a vector along the two joint centres of the link of length l_2. Therefore, when the three links of length l_2 are parallel, we have

$$\mathbf{v}_1 = \pm\mathbf{v}_2 = \pm\mathbf{v}_3 \tag{63}$$

and the second column of $\mathbf{A}$ is a multiple of the first one. In this case, the nullspace of $\mathbf{A}$ represents the set of pure translations of the gripper along a direction orthogonal to $\mathbf{v}_i$, i.e., orthogonal to the three links of length l_2. A velocity of the gripper of that nature would produce motor rates of zero and a force applied to the gripper in that direction cannot be balanced by the actuators.

It is to be noticed that the results presented above for the second kind of singularity of the revolute-based planar three-degree-of-freedom manipulator are in full agreement with the ones reported in [12].

The third kind of singularity is characterized by the undeterminacy of eq.(43). In other words, the manipulator architecture allows for the vanishing of both det($\mathbf{A}$) and det($\mathbf{B}$).

As mentioned above, this singularity is not only configuration- but also architecture-dependent. For the planar manipulator studied here, two situations may produce it. One of these two cases happens when we have:

$$l_1 = \frac{\sqrt{3}}{3} \quad \text{and} \quad l_2 = l_3 \tag{64}$$

With these constraints on the link lengths, we can reach a configuration where the tip of each of the three links of lengths l_1 meet at the centroid of the base triangle which coincides with the centroid of the gripper, since $l_2 = l_3$. The gripper can then undergo arbitrary rotations about its centroid while the motors remain at rest. This indeterminacy is due to the zeroing of both the c_i's and the d_i's when the gripper is oriented such that $\phi = 0$. At this particular point, both the first and second kinds of singularities meet.

The second case of degeneracy of the manipulator requires the following conditions:

$$l_1 = l_2 \quad \text{and} \quad l_3 = \frac{\sqrt{3}}{3} \tag{65}$$

In that case, the gripper is of the same size as the base triangle. Therefore, when the three vertices of the gripper are located at the centroid of the motors, and when angle ϕ is equal to zero, the motors can undergo arbitrary rotations while the gripper remains at rest. Again, the first two kinds of singularities meet here, i.e., when angles θ_1, θ_2, and θ_3 take on the values $-150°$, $-30°$, and $90°$ respectively, then both the c_i's and the d_i's are equal to zero.

6 Example 4: Spherical Three-Degree-of-Freedom Parallel Manipulator

This type of parallel manipulator was described in [26] and studied in detail in [27]. A spherical parallel manipulator can be applied as an orientation wrist in robotics. Applications outside of robotics, that could be mentioned, are mechanisms for the orientation of machine-tool beds and workpieces, solar panels, antennas, etc. Hence the motivation to study this type of kinematic chains.

A spherical parallel manipulator is represented in Fig. 9, all of whose joints are of the revolute type, and the three motors M_1, M_2, M_3 are fixed. The manipulator consists of a kinematic chain with three closed loops, namely M_1DABEM_2, M_2EBCFM_3, and M_3FCADM_1, and the gripper is rigidly attached to triangle ABC. Again, only two of the loops are independent. As for the case of the planar manipulator, a symmetric layout has been chosen here. By symmetry, then, the axes of the motors will be located in a common plane, intersecting a point defining the *centre* of the spherical manipulator. Moreover, the joints attached to the gripper have the same relative orientation, and the link angles will be the same for each leg, i.e.,

$$\alpha_i = \alpha_i' = \alpha_i'', \quad i = 1, 2 \tag{66}$$

The expression of the Jacobian matrix of this manipulator is now recalled from [27]. Let us define $\mathbf{u}_i$ as a unit vector along the axis of the ith input motor, and $\mathbf{v}_i$ as a unit vector along the axis of the revolute joints connecting the gripper and the adjacent link and $\mathbf{w}_i$, a unit vector along the axes of the intermediate revolute pairs of each leg, for $i = 1, 2, 3$. We then write the differential kinematic relations as:

$$\mathbf{A}\omega + \mathbf{B}\dot{\theta} = \mathbf{0} \tag{67}$$

where ω is the angular velocity of the end effector and $\dot{\theta}$ is the vector of actuated joint rates. Matrices $\mathbf{A}$ and $\mathbf{B}$ are

$$\mathbf{A} = \begin{bmatrix} (\mathbf{w}_1 \times \mathbf{v}_1)^T \\ (\mathbf{w}_2 \times \mathbf{v}_2)^T \\ (\mathbf{w}_3 \times \mathbf{v}_3)^T \end{bmatrix} \tag{68}$$

$$\mathbf{B} = \mathrm{diag}\left(\mathbf{w}_1 \times \mathbf{u}_1 \cdot \mathbf{v}_1,\, \mathbf{w}_2 \times \mathbf{u}_2 \cdot \mathbf{v}_2,\, \mathbf{w}_3 \times \mathbf{u}_3 \cdot \mathbf{v}_3\right) \tag{69}$$

The first kind of singularity is known to lie on the boundary of the workspace and appears whenever $\det(\mathbf{B}) = 0$. The conditions under which this kind of singularity arises can be obtained from the expression of $\mathbf{B}$ given above, i.e.,

$$(\mathbf{w}_i \times \mathbf{u}_i) \cdot \mathbf{v}_i = 0, \qquad i = 1 \text{ or } 2 \text{ or } 3 \tag{70}$$

Equation (70) states that vectors $\mathbf{u}_i$, $\mathbf{v}_i$, and $\mathbf{w}_i$ are coplanar, i.e., that the corresponding leg is totally unfolded or folded. When such a configuration is attained, a certain set of velocitites of the gripper cannot be produced. This set of velocities corresponds to the motions of the gripper that involve a velocity of the point of attachment of the fully extended or folded leg to

the gripper along the direction of the leg. However, a torque applied to the gripper that would involve a force along the fully extended or folded leg would not produce any torque at the actuators but would be resisted by the manipulator.

The second kind of singularity—which occurs when $\det(\mathbf{A}) = 0$—appears in configurations in which nonzero angular velocities of the gripper are possible even if the three motors are locked. For the spherical manipulator, the condition under which $\det(\mathbf{A})=0$ can be derived from expression (68). Since, by definition, vectors $\mathbf{w}_i$ and $\mathbf{v}_i$ cannot be identical, then this condition is that the three vectors $(\mathbf{w}_i \times \mathbf{v}_i, i = 1, 2, 3)$ are coplanar. Since $\mathbf{v}_1, \mathbf{v}_2$ and $\mathbf{v}_3$ are coplanar, this condition states that the three planes defined, respectively, by the pairs of vectors $(\mathbf{v}_i, \mathbf{w}_i)$, for $i = 1, 2, 3$, either have a common intersection along an axis or are identical. This corresponds to configurations in which the links of dimension α_2 either lie on the plane of the gripper or are orthogonal to this plane. In each of these cases, a velocity of the gripper that leaves the actuators at rest is possible and there exists a torque which, when applied to the gripper, could not be balanced by the actuators.

Two sets of spherical manipulators for which the third kind of singularity can occur are identified here, the second one being a subset of the first one.

First, for the set of spherical manipulators having $\alpha_1 = \alpha_2$, the configuration in which we have $\mathbf{u}_i = \mathbf{v}_i$ for $i = 1, 2, 3$ is attainable and it constitutes a special case because condition (70) is verified for all three legs. Therefore, in this case, any motion of the input links will not affect the gripper since the former are just rotating, together with the intermediate link, around the axis defined by vectors $\mathbf{u}_i = \mathbf{v}_i$, leaving the gripper at rest. The rank of $\mathbf{B}$ is then equal to zero in this configuration, i.e., none of the three Cartesian components of ω can be produced in the said configuration. Moreover, if $\theta_1 = \theta_2 = \theta_3 = 0$ or if $\theta_1 = \theta_2 = \theta_3 = \pi/2$, from the discussion above, the first and the second kinds of singularities meet.

Furthermore, if we have, more specifically, $\alpha_1 = \alpha_2 = \pi/2$, all the configurations for which $\mathbf{v}_1, \mathbf{v}_2, \mathbf{v}_3$ are coplanar to $\mathbf{u}_1, \mathbf{u}_2, \mathbf{u}_3$, are singular. This set of configurations is characterized by the fact that the gripper can be rotated around the axis orthogonal to the plane defined by vectors $\mathbf{u}_1, \mathbf{u}_2, \mathbf{u}_3$ without moving the input links.

7 Example 5: Spatial Six-Degree-of-Freedom Parallel Manipulator

This type of device is very well known for its application in flight simulators and several authors have been considering using it as a robotic manipulator [12,28,29]. The notation used here is consistent with the one used in [22]. Therefore, the manipulator is as shown in Fig. 10. The points of attachment of the legs, i.e., the centers of the spherical joints, are located on the base and on the platform as shown in Figs. 11 and 12, i.e., on the circumference of circles of radii R_B (base) and R_P (platform), respectively. The points of attachment are grouped by pairs which are uniformly spaced along the circle and they are denoted by B_i and P_i for $i = 1, \ldots, 6$. Furthermore, the position vectors of point B_i and P_i are given by vectors $\mathbf{b}_i$ and $\mathbf{p}_i$, for $i = 1, \ldots, 6$, respectively, in a coordinate frame fixed to the base of the manipulator. The position vector of point P_i in a coordinate frame fixed to the platform is, in turn, given by vector $\mathbf{p}'_i$. We can write:

$$\mathbf{b}_i = \begin{bmatrix} R_B \cos\theta_i \\ R_B \sin\theta_i \\ 0 \end{bmatrix}, \quad i = 1, \ldots, 6 \tag{71}$$

where

$$\theta \equiv \begin{bmatrix} \theta_1 \\ \theta_2 \\ \theta_3 \\ \theta_4 \\ \theta_5 \\ \theta_6 \end{bmatrix} = \begin{bmatrix} \phi_B \\ 2\pi/3 - \phi_B \\ 2\pi/3 + \phi_B \\ 4\pi/3 - \phi_B \\ 4\pi/3 + \phi_B \\ -\phi_B \end{bmatrix} \tag{72}$$

and

$$\mathbf{p}'_i = \begin{bmatrix} R_P \cos\eta_i \\ R_P \sin\eta_i \\ 0 \end{bmatrix}, \quad i = 1, \ldots, 6 \tag{73}$$

where

$$\eta \equiv \begin{bmatrix} \eta_1 \\ \eta_2 \\ \eta_3 \\ \eta_4 \\ \eta_5 \\ \eta_6 \end{bmatrix} = \begin{bmatrix} \phi_P \\ 2\pi/3 - \phi_P \\ 2\pi/3 + \phi_P \\ 4\pi/3 - \phi_P \\ 4\pi/3 + \phi_P \\ -\phi_P \end{bmatrix} \tag{74}$$

Moreover, we denote the position vector of the center of the platform, i.e., the center of the circle in Fig. 12 by $\mathbf{x}$, while the rotation matrix defining the orientation of the platform is denoted by $\mathbf{Q}$. Hence, the solution of the inverse kinematic problem can be written as

$$c_i = \sqrt{U_i^2 + V_i^2 + W_i^2}, \quad i = 1, \ldots, 6 \tag{75}$$

where

$$U_i = x + q_{11} R_P \cos\eta_i + q_{12} R_P \sin\eta_i - R_B \cos\theta_i \tag{76}$$

$$V_i = y + q_{21} R_P \cos\eta_i + q_{22} R_P \sin\eta_i - R_B \sin\theta_i \tag{77}$$

$$W_i = z + q_{31} R_P \cos\eta_i + q_{32} R_P \sin\eta_i \tag{78}$$

in which, c_i is the length of the ith leg and variables x, y, z and q_{ij} for $i, j = 1, 2, 3$ are the components of the Cartesian coordinates, i.e., vector $\mathbf{x}$ and matrix $\mathbf{Q}$, respectively.

The velocity relation (2) can be written as

$$\mathbf{A}\dot{\mathbf{y}} + \mathbf{B}\dot{\mathbf{c}} = \mathbf{0} \tag{79}$$

where $\dot{\mathbf{c}}$ and $\dot{\mathbf{y}}$ are defined as $\dot{\mathbf{c}} = [\dot{c}_1, \ldots, \dot{c}_6]^T$ and $\dot{\mathbf{y}} = [\dot{x}, \dot{y}, \dot{z}, \omega_1, \omega_2, \omega_3]^T$ in which the angular velocity of the platform is defined as $\omega = [\omega_1, \omega_2, \omega_3]^T$. Also, we define a set of vectors $\mathbf{w}_i, i = 1, \ldots, 6$ as

$$\mathbf{w}_i = c_i \mathbf{e}_i = \begin{bmatrix} U_i \\ V_i \\ W_i \end{bmatrix}, \quad i = 1, \ldots, 6 \tag{80}$$

where $\mathbf{e}_i$ is a unit vector along the ith leg, pointing from the base to the platform. Hence we have:

$$\mathbf{A} = \begin{bmatrix} \mathbf{a}_1^T \\ \mathbf{a}_2^T \\ \vdots \\ \mathbf{a}_6^T \end{bmatrix} \tag{81}$$

where

$$\mathbf{a}_i = \begin{bmatrix} \mathbf{w}_i^T, & \{(\mathbf{Q}\mathbf{p}_i') \times \mathbf{w}_i\}^T \end{bmatrix}^T, \quad i = 1, \ldots, 6 \tag{82}$$

and

$$\mathbf{B} = \mathrm{diag}(c_1, \ldots, c_6) \tag{83}$$

If we assume that the prismatic actuators of the manipulator have an infinite range of motion, the result is an infinitely large workspace and the

first kind of singularity occurs only when one of the actuators has a length of zero, i.e.,

$$c_i = 0 \qquad i = 1 \quad \text{or} \quad 2 \quad \text{or} \ldots 6 \tag{84}$$

From eq.(83), it is readily seen that this situation produces a singular **B** matrix. This is so because the direction of the prismatic joint is undefined in these configurations.

However, in a real manipulator, the actuators have a finite range of motion, i.e.,

$$c_{\min} \leq c_i \leq c_{\max} \tag{85}$$

and where $c_{\min}$ is, in general, different from zero. In this case, the first kind of singularity occurs when one of the actuators reaches one of its limits, i.e.

$$c_i = c_{\min} \quad \text{or} \quad c_i = c_{\max}, \quad i = 1 \quad \text{or} \quad 2 \quad \text{or} \ldots 6 \tag{86}$$

which corresponds to the limit of the workspace. Since one of the actuators cannot move further in one direction, a certain set of gripper (platform) velocities cannot be produced and a certain combination of forces and moments applied to the gripper does not affect the actuators.

The analysis of the second kind of singularity is more complicated for it entails finding the conditions under which matrix **A** is singular. This is still a subject of current research [12,28–30]. In reference [29], Grassmann geometry is used to identify the singularities. This geometrical approach, which is similar to the use of screw theory is justified here because it can be seen from eq.(82) that the rows of matrix **A** are unnormalized Plücker coordinates of lines along the legs of the platform. In the formulation of equations presented here, matrix **A** is slightly different from the Jacobian matrix used in the other references [12,28,29] because the introduction of matrix **B** allowed us to eliminate the denominators in the Jacobian matrix—this is why we obtain *unnormalized* Plücker coordinates—and hence, the expression obtained for the determinant is a little simpler. However, it seems that for this case, geometrical approaches have so far produced better results than analytical ones.

The third kind of singularity occurs when the following conditions are verified:

$$R_P = R_B \quad \text{and} \quad \theta = \eta \tag{87}$$

With this special geometry and in a configuration where all actuator lengths are the same, the platform can undergo motions of a finite amplitude even if the actuators are locked. Indeed, in such a situation, all legs are

parallel and the platform can undergo translations that would arbitrarily position the center of the platform on the surface of a sphere of radius equal to the length of one leg and centered at the center of the base circle. The orientation of the platform is such that $\mathbf{Q} = \mathbf{1}$ and is preserved throughout this motion. In this case, the first two kinds of singularities can meet when all legs have the same length and reach one of their limits.

8 Conclusion

A general classification of the different kinds of singularities encountered in closed-loop kinematic chains was given. Three main kinds of singularities were identified and their physical significance was described. The classification was illustrated through a series of examples which included closed-loop mechanisms and parallel manipulators. The results obtained here can be used for the identification of the singularities of these mechanical systems which is an important issue in design and control.

9 Acknowledgements

The research work reported here was completed under an NSERC (Natural Sciences and Engineering Research Council of Canada) postgraduate scholarship granted to the first author and under NSERC Research Grant # A-4532 and FCAR (Fonds pour la formation de chercheurs et l'aide à la recherche, of Québec) Research Grant # EQ-3072.

References

[1] Z.C. Lai and D.C.H. Yang, 'A new method for the singularity analysis of simple six link manipulators', *The International Journal of Robotics Research*, Vol. 5, No. 2, pp. 66–74, 1987.

[2] F.L. Litvin and V. Parenti Castelli, 'Configurations of robot manipulators and their identification, and the execution of prescribed trajectories Part-I: Basic concepts', *ASME Journal of Mechanisms, Transmissions, and Automation in Design*, Vol. 107, No. 2, pp. 170–178, 1985.

[3] K.J. Waldron, S.L. Wang and S.J. Bolin, 'A study of the Jacobian matrix of serial manipulators', *ASME Journal of Mechanisms, Trans-*

missions, and Automation in Design, Vol. 107, No. 2, pp. 230–237, 1985.

[4] F.L. Litvin, T. Costopoulos, V. Parenti Castelli, M. Shaheen and Y. Yukishige, 'Configurations of robot manipulators and their identification, and the execution of prescribed trajectories Part-II: Investigation of manipulators having five, seven and eight degrees of freedom', *ASME Journal of Mechanisms, Transmissions, and Automation in Design*, Vol. 107, No. 2, pp. 179–188, 1985.

[5] F.L. Litvin, Z. Yi, V. Parenti Castelli and C. Innocenti, 'Singularities, configurations, and displacement functions for manipulators', *The International Journal of Robotics Research*, Vol. 5, No. 2, pp. 52–65, 1986.

[6] K.H. Hunt, 'Special configurations of robot-arms via screw theory- Part I: The Jacobian and its matrix cofactors', *Robotica*, Vol. 4, pp. 171–179, 1986.

[7] K.H. Hunt, 'Special configurations of robot-arms via screw theory- Part II: Available end-effector displacements', *Robotica*, Vol. 5, pp. 17–22, 1987.

[8] S.-L. Wang, and K.J. Waldron, 'A study of the singular configurations of serial manipulators', *ASME Journal of Mechanisms, Transmissions, and Automation in Design*, Vol. 109, No. 1, pp. 14–20, 1987.

[9] K. Sugimoto, J. Duffy and K.H. Hunt, 'Special configurations of spatial mechanisms and robot arms', *Mechanism and Machine Theory*, Vol. 17, No. 2, pp. 119–132, 1982.

[10] J. Eddie Baker, 'Screw system algebra applied to special linkage configurations', *Mechanism and Machine Theory*, Vol. 15, No. 4, pp. 255–265, 1980.

[11] F.L. Litvin, J. Tan, P. Fanghella and S. Wu, 'Singularities in motion and displacement functions for the RCRCR, RCRRC and RSRC linkages Part-I: Basic concepts', *Proceedings of the 13th ASME Design Automation Conference*, pp. 267–278, Boston, 1987.

[12] K.H. Hunt, 'Structural kinematics of in-parallel-actuated robot arms', *ASME Journal of Mechanisms, Transmissions, and Automation in Design*, Vol. 105, No. 4, pp. 705–712, 1983.

[13] K.H. Hunt, 'Kinematic Geometry of Mechanisms', *Clarendon Press*, Oxford, 1978.

[14] H. Asada and K. Youcef-Toumi, 'Analysis and design of a direct-drive arm with a five-bar-link parallel drive mechanism', *ASME Journal of Dynamic Systems, Measurements, and Control*, Vol. 106, No. 3, pp. 225–230, 1984.

[15] J. Eddie Baker, 'On the investigation of extrema in linkage analysis using screw system algebra', *Mechanism and Machine Theory*, Vol. 13, No. 3, pp. 333–343, 1978.

[16] J. Eddie Baker, 'Limit positions of spatial linkages via connectivity sum reduction' *Journal of Mechanical Design*, Vol. 101, No. 3, pp. 504–508, 1979.

[17] J. Eddie Baker and K.J. Waldron, 'Limit positions of spatial linkages via screw theory', *ASME paper* no. 74-DET-107, 1974.

[18] H.S. Yan and L.I. Wu, 'The stationary configurations of planar six-bar kinematic chains', *Mechanism and Machine Theory*, Vol. 23, No. 4, pp. 287–293, 1988.

[19] K.J. Waldron and K.H. Hunt, 'Series-parallel dualities in actively coordinated mechanisms', *Robotics Research 4*, eds. R. Bolles and B. Roth, pp. 175–181, 1988.

[20] C.H. Chiang, 'Kinematics of spherical mechanisms', Cambridge University Press, 1988.

[21] G.S. Sandor, D. Kohli and X. Zhuang, 'Synthesis of RSSR-SRR spatial motion generator mechanism with prescribed crank rotations for three and four finite positions', *Mechanism and Machine Theory*, Vol. 20, No. 6, pp. 503–519, 1985.

[22] C. Gosselin, 'Kinematic analysis, optimization and programming of parallel robotic manipulators', Ph.D. Thesis, Dept. of Mech. Eng., McGill University, Montréal, Québec, Canada, 1988.

[23] R. Russell, 'Kinematic optimization of lower-pair clutch mechanisms', M. Eng. Project, Dept. of Mech. Eng., McGill University, Montréal, Québec, Canada, 1988.

[24] J. Angeles and A. Bernier, 'A general method of four-bar linkage mobility analysis', *ASME Journal of Mechanisms, Transmissions, and Automation in Design*, Vol. 109, No. 2, pp. 197–203, 1987.

[25] C. Gosselin and J. Angeles, 'The optimum kinematic design of a planar three-degree-of-freedom parallel manipulator', *ASME Journal of Mechanisms, Transmissions, and Automation in Design*, Vol. 110, No. 1, pp. 35–41, 1988.

[26] H. Asada and J.A. Cro Granito, 'Kinematic and Static characterization of wrist joints and their optimal design', *Proceedings of the IEEE Conf. on Robotics and Automation*, St-Louis, pp. 244–250, 1985.

[27] C. Gosselin and J. Angeles, 'The optimum kinematic design of a spherical three-degree-of-freedom parallel manipulator', *ASME Journal of Mechanisms, Transmissions, and Automation in Design*, Vol. 111, No. 2, pp. 202–207, 1989.

[28] E.F. Fichter, 'A Stewart platform-based manipulator: general theory and practical construction', *The International Journal of Robotics Research*, Vol. 5, No. 2, pp. 157–182, 1986.

[29] J.P. Merlet, 'Parallel manipulators, Part II: Theory, singular configurations and Grassmann geometry', Technical Report # 791, INRIA, France, 1988.

[30] F. Behi, 'Kinematic analysis for a six-degree-of-freedom 3-PRPS parallel mechanism', *IEEE Journal of Robotics and Automation*, Vol. 4, No. 5, pp. 561–565, 1988.

LIST OF FIGURES

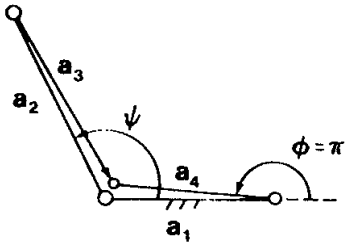

Fig. 1. Four-bar linkage degeneracy illustrating a singularity of the third kind.

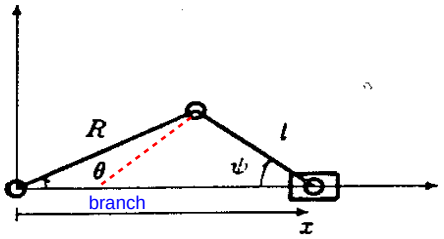

Fig. 2. Planar *RRRP* mechanism.

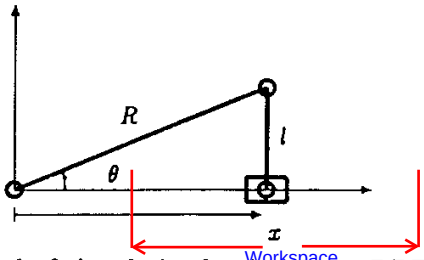

Fig. 3. Second kind of singularity for the planar *RRRP* mechanism.

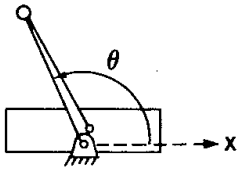

Fig. 4. Singularity of the third kind for the planar *RRRP* mechanism.

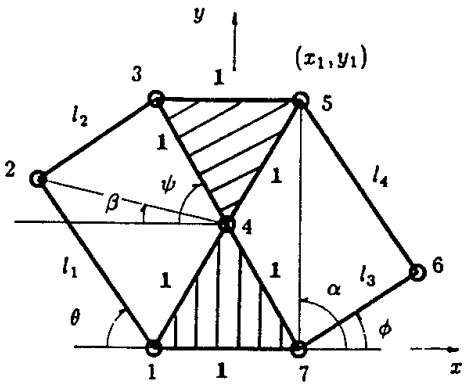

Fig. 5. Watt's linkage.

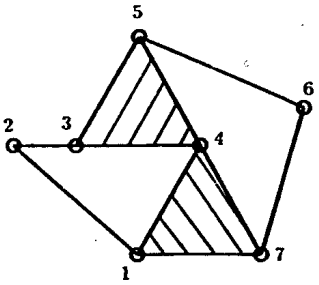

Fig. 6. Second kind of singularity for Watt's linkage.

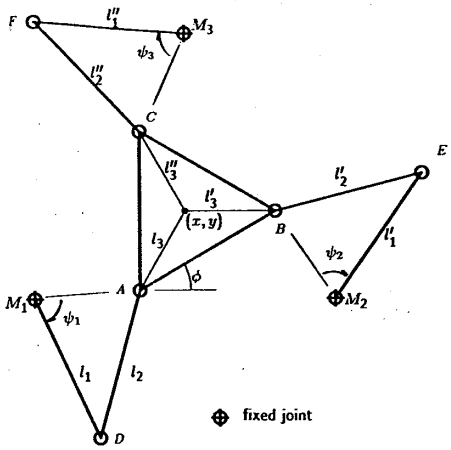

Fig. 7. Planar three-degree-of-freedom parallel manipulator with revolute actuators.

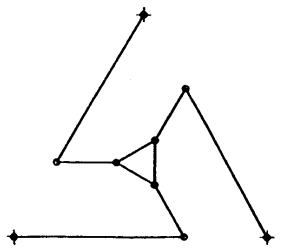

Fig. 8. Example of the second kind of singularity for the planar three-degree-of-of-freedom parallel manipulator.

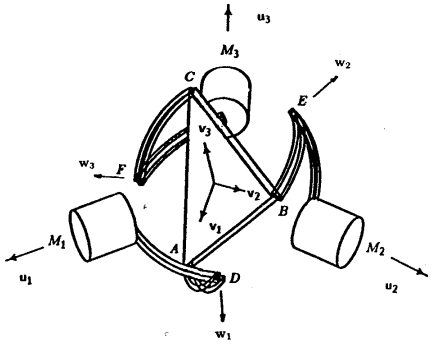

Fig. 9. Spherical three-degree-of-freedom parallel manipulator.

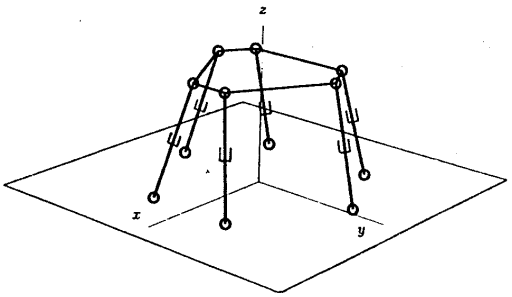

Fig. 10. Spatial six-degree-of-freedom parallel manipulator.

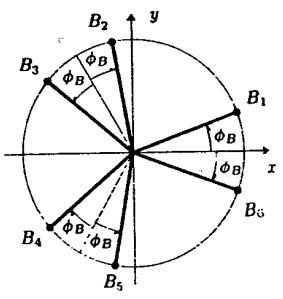

Fig. 11. Position of the joints on the base.

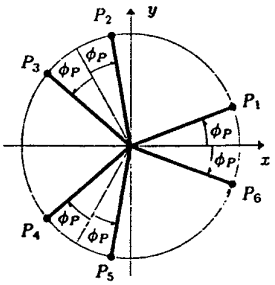

Fig. 12. Position of the joints on the platform.